E-Article

Effect of Stressors on the Carrying Capacity of Spatially Distributed Metapopulations

Bo Zhang,[1,2] Donald L. DeAngelis,[3] Wei-Ming Ni,[4] Yuanshi Wang,[5] Lu Zhai,[6] Alex Kula,[1] Shuang Xu,[1] and J. David Van Dyken[1,*]

1. Department of Biology, University of Miami, Coral Gables, Florida 33146; 2. Department of Environmental Science and Policy, University of California, Davis, California 95616; 3. Wetland and Aquatic Research Center, US Geological Survey, Gainesville, Florida 32653; 4. School of Mathematics, University of Minnesota, Minneapolis, Minnesota 55455; Center for Partial Differential Equations, East China Normal University, Shanghai, China; and Chinese University of Hong Kong, Shenzhen, China; 5. School of Mathematics and Computational Science, Sun Yat-sen University, Guangzhou, China; 6. Department of Natural Resource Ecology and Management, Oklahoma State University, Stillwater, Oklahoma 74078

Submitted December 2, 2019; Accepted February 3, 2020; Electronically published June 10, 2020

Online enhancements: supplemental PDF. *Dryad data:* https://doi.org/10.25338/B8090K.

abstract: Stressors such as antibiotics, herbicides, and pollutants are becoming increasingly common in the environment. The effects of stressors on populations are typically studied in homogeneous, nonspatial settings. However, most populations in nature are spatially distributed over environmentally heterogeneous landscapes with spatially restricted dispersal. Little is known about the effects of stressors in these more realistic settings. Here, we combine laboratory experiments with novel mathematical theory to rigorously investigate how a stressor's physiological effect and spatial distribution interact with dispersal to influence population dynamics. We prove mathematically that if a stressor increases the death rate and/or simultaneously decreases the population growth rate and yield, a homogeneous distribution of the stressor leads to a lower total population size than if the same amount of the stressor was heterogeneously distributed. We experimentally test this prediction on spatially distributed populations of budding yeast (*Saccharomyces cerevisiae*). We find that the antibiotic cycloheximide increases the yeast death rate but reduces the growth rate and yield. Consistent with our mathematical predictions, we observe that a homogeneous spatial distribution of cycloheximide minimizes the total equilibrium size of experimental metapopulations, with the magnitude of the effect depending predictably on the dispersal rate and the geographic pattern of antibiotic heterogeneity. Our study has implications for assessing the population risk posed by pollutants, antibiotics, and global change and for the rational design of strategies for employing toxins to control pathogens and pests.

Keywords: consumer-resource model, spatially heterogeneous parameters, patchy environment, laboratory experiments, spatial ecology, movement ecology.

* Corresponding author; email: vandyken@bio.miami.edu.
ORCIDs: Zhang, https://orcid.org/0000-0002-5313-0816.

Am. Nat. 2020. Vol. 196, pp. E46–E60.
DOI: 10.1086/709293

Introduction

Natural populations are often exposed to various environmental stressors, that is, factors that negatively impact vital rates. Stressors may be a natural part of the landscape or may be introduced into the environment either accidentally or deliberately by human activity (Tilman and Lehman 2001; Bond-Lamberty et al. 2014; Ha et al. 2014). A fundamental problem in ecology is determining how environmental stressors influence population dynamics (Konopka 2009). Much laboratory work and fieldwork has quantified the effects of stressors on individual vital rates, such as mortality and fecundity (Lefebvre et al. 1999). Other work has then quantified the effects of stressors on population dynamics in a single field or laboratory population (Hendriks et al. 2005). However, much less is understood about the effects of stressors at the global level (i.e., metapopulation, defined as the sum of abundances of individuals over all local populations), specifically when stressors are heterogeneously distributed over a species range (Spromberg et al. 1998; Fritsch et al. 2010; Genin et al. 2018).

Most stressors are heterogeneously distributed over a species range. This is true, in particular, for anthropogenic sources of stress, which include accidental (undesirable) introductions into the environment and those stressors that are deliberately introduced into the environment as a form of species control. Industrial pollutants, for example, are unintentional by-products of human activity that are usually spatially localized around their source (Solis-Weiss et al. 2004). Herbicides are deliberately introduced into the environment to control pests. Applications of these agents are usually not distributed uniformly over the pest species range, though, because there are often budgetary constraints or political differences among regions where control is being

applied that influence the level of application. For example, measures to control the spread of infectious diseases such as Zika and malaria by reducing mosquito populations have always been spatially restricted to particular regions of the mosquito's range (Ferguson et al. 2016). Meanwhile, the deliberate introduction of herbicides can have spillover effects on nontarget species, as these agents spread via air (Yao et al. 2006) and run off into adjacent land and waterways (Hunt et al. 2006). Thus, while some stressors, such as rising temperature and CO_2, are more likely to occur homogeneously across space, at least on some spatial scales (Mann et al. 1998), anthropogenic stressors are often heterogeneously distributed over the ranges of animal and plant species.

Spatial environmental heterogeneity greatly complicates efforts to predict population dynamics (Reiners and Driese 2001; Van Dyken and Zhang 2019). For this reason, little is known either theoretically or empirically about how populations are influenced by the geographic distribution of stressors. Predicting how populations will respond to stressors is substantially complicated by the fact that most species in nature live in populations with a spatially restricted dispersal of individuals (Skellam 1951; Andow et al. 1993; Kot et al. 1996; Hastings et al. 2005). With spatially restricted dispersal, individuals cannot disperse freely over the entire spatial regions but rather are constrained by time, energy, and movement ability such that the probability of dispersing to nearby regions is higher than the probability of dispersing to far away regions. Because of this spatially restricted movement, an individual does not equally experience all environments over the species range. Thus, if the environment is heterogeneous on a coarse scale (Levins 1968), individuals within a species will differ in their fitness simply as a result of different environmental experiences. Spatial regions may then vary in the number of individuals they can support, creating heterogeneity in population density over space.

A growing body of theory based on patch equations with logistic growth (eqq. [1]) has demonstrated that the interaction between resource heterogeneity and dispersal in spatially structured populations can both quantitatively and qualitatively alter population dynamics (Holt 1985; Freedman et al. 1987; Law et al. 2003; Lou 2006; Herbener et al. 2012):

$$\frac{dU_1}{dt} = r_1\left(1 - \frac{U_1}{K_1}\right)U_1 - DU_1 + DU_2, \qquad (1a)$$

$$\frac{dU_2}{dt} = r_2\left(1 - \frac{U_2}{K_2}\right)U_2 - DU_2 + DU_1, \qquad (1b)$$

where U_1 and U_2 are the population size in patch 1 and 2, respectively; r is the growth rate; K is the carrying capacity; and D is the dispersal rate between the two patches.

Theory based on equations of this form predicts that environmental heterogeneity, as modeled by spatial variation in the parameters r and/or K among patches, increases metapopulation abundance when individuals disperse among patches (DeAngelis et al. 2016). This remarkable theoretical result has been called a paradox (Arditi et al. 2015). However, the logistic equation is not well suited to mapping physiology, a biological/mechanistic feature, to the phenomenological parameters of r and K. In addition, the logistic model does not disentangle the effects of fecundity and mortality on population growth rate, as both effects are aggregated into the composite parameter r (which equals births minus deaths). Since stressors often act to either decrease reproduction or increase death (Hendriks et al. 2005) and since deaths may result from density-independent or density-dependent causes, the logistic model conflates all of these effects, potentially concealing important distinctions.

As an alternative to the logistic approach, it has recently been demonstrated that a bottom-up approach with a metapopulation of consumers utilizing explicit resources (MacArthur 1972; Tilman 1982) is more suitable for describing the effects of environmental heterogeneity (Zhang et al. 2017). Specifically, when population growth is modeled using a mechanistic, bottom-up approach with explicit resources, the so-called paradox of heterogeneity vanishes (Zhang et al. 2017; Ruiz-Herrera and Torres 2018). That is, in direct contradiction to predictions based on the phenomenological spatial logistic equation (eqq. [1]), consumer-resource models predict that resource heterogeneity decreases metapopulation size rather than increasing it. Experimental work by Zhang et al. (2017) confirmed the predictions of the consumer-resource models, demonstrating empirically that the paradox did not occur in their experimental system. However, this work has been restricted to a heterogeneity of resources that have a positive effect on growth, whereas environmental stressors have a negative effect on growth. Specifically, stressors can have alternative modes of action, by which we mean that they can target different components of fitness, reducing individual fertility, survival, and/or assimilation of resources. It therefore remains an open question whether predictions based on mechanistic bottom-up models of spatial populations with heterogeneity in stressors will differ from those made in previous logistic-based models.

Therefore, here we develop novel mathematical theory that we then test using high-throughput experiments on spatially dispersing experimental metapopulations of the budding yeast (*Saccharomyces cerevisiae*), subject to experimental manipulation of the dispersal rate and the spatial distribution of the amount of a stressor (specifically, the antibiotic drug cycloheximide). This experimental system has been shown to be a good empirical model for testing ecological theory of spatially structured metapopulations

(Zhang et al. 2017). Our goal then is first to mathematically analyze a mechanistic consumer-resource model of spatial metapopulation dynamics in environments with heterogeneous and homogenous distributions of a stressor (the environment is otherwise homogeneous). We then use a previously validated experimental setup (Sen Datta et al. 2013; Gandhi et al. 2016) to rigorously test our theoretical predictions in carefully controlled laboratory conditions. Ultimately, we ask: How does the spatial distribution of a stressor interact with dispersal to determine the impact of a stressor on metapopulation size?

Mathematical Theory

We model a randomly dispersing consumer metapopulation occupying a one-dimensional spatial habitat composed of n discrete, equal-sized patches. We assume that symmetric dispersal occurs between neighboring patches except for patches 1 and n at the ends, for which there is dispersal only to patches 2 and $n - 1$, respectively. This is a linear stepping-stone model (Wright 1943; Kimura and Weiss 1964). In the continuum limit, this population structure can be conceptualized as spatial diffusion. Although simplistic, the ability of linear diffusion and stepping-stone models to explain patterns in nature is now well established, with good correspondence between models and data for many natural populations (Skellam 1951; Andow et al. 1993; Kot et al. 1996; Hastings et al. 2005).

We now superimpose this spatial setting onto a consumer-resource model of local population dynamics. We assume that growth of the consumer metapopulation is determined by a single renewable limiting resource, which has the same input rate at every patch in space. We model the effect of a generic stressor, such as a chemical toxicant, as a negative effect on one or a combination of the parameters: the asymptotic reproduction rate (or maximum population growth rate) at infinite resources, $r_{\max}$; the number of consumers supported per unit resource (i.e., the yield), γ; or a positive effect on the density-independent death rate, m, and the density-dependent death rate, g. We assume that the effect of the stressor is linearly proportional to the amount of stressor. The assumption of linear effects on these parameters may be unrealistic in some cases but nonetheless provides a valid first-order approximation. These four parameter values can vary among patches, determined by the local stressor amount. The model is designed to apply to the experiments described below but can be applied to stressors affecting populations on spatial scales up to and including the landscape scale. But for those larger scales, we must assume that the increase in mortality rate or the loss of growth rate is linearly proportional to the amount of stressor. This may apply most appropriately to a deliberately applied stressor. But it might not apply to some pollutants; that is, as the concentration of a pollutant decreases (or dilutes), its effect on mortality or growth may decrease at a greater than linear rate.

The spatial-temporal dynamics of the consumer-resource system can be written in general n-patch form as follows (see supplement 1; supplements 1–6 are available online in the supplemental PDF):

$$\frac{dU_i}{dt} = \frac{r_{\max,i} N_i U_i}{K_S + N_i} - m_i U_i - g_i U_i^2 - D\left(U_i - \frac{1}{2}U_{i-1} - \frac{1}{2}U_{i+1}\right) \quad (i = 2, n-1), \tag{2a}$$

$$\frac{dN_i}{dt} = N_{\text{input},i} - \eta N_i - \frac{r_{\max,i} N_i U_i}{\gamma_i (K_S + N_i)} \quad (i = 1, n), \tag{2b}$$

where U_i is the consumer (yeast) biomass in patch i, N_i is the nutrient, K_S is the half-saturation coefficient, D is the dispersal rate, $N_{\text{input},i}$ is the nutrient input, and η is the nutrient dilution rate. In equation (2a), for $i = 1$ and $i = n$, dispersal occurs only with $i = 2$ and $i = n - 1$, respectively. For ease of analysis, two submodels were analyzed separately in Zhang et al. (2017) and here: model 1 (chemostat), for which $\eta = 0$, $m_i = 0$, and $g_i > 0$ for all i; and model 2, for which $\eta = 1$, $m_i > 0$, and $g_i = 0$ for all i (see supplement 1 for an explanation of the rationale for the two models).

Using these models of a consumer and an exploitable resource in a spatial environment, we test whether a specific amount of stressor that can reduce either $r_{\max}$ or γ (or both together) or that can increase m or g is more effective when it occurs as homogeneously or heterogeneously distributed among the patches. Effectiveness is measured by the ability to minimize the metapopulation equilibrium total realized asymptotic population abundance (TRAPA). We test this for both a dispersing and a nondispersing population for both models.

We analyze for effects of stressor on parameters $r_{\max}$ and γ for both models as well as on g in model 1 and m in model 2. We assume that the effect of the stressor on each parameter in a given patch is proportional to the amount of stressor in that patch. Suppose that there is some total amount T that has an effect $e(T)$. Then the effect on a given generic parameter—say, y_i—would be, for uniform application in two patches (1 and 2) and assuming a negative effect, $y_1 = y_2 = y_{\text{homogeneous}} = y_{\text{baseline}} - e_y(T/2)$, where y_{baseline} is y in the absence of stressor. If the stressor is applied only to patch 1, then $y_1 = y_{\text{baseline}} - e_y(T)$ and $y_2 = y_{\text{baseline}}$. These are simple assumptions, but they can give at least first-order results. For mathematical analysis and simulation it was more convenient to take $y_{\text{homogeneous}}$ as the

baseline, so that $y_1 = y_{\text{homogeneous}} + e_y(T/2)$ and $y_2 = y_{\text{homogeneous}} - e_y(T/2)$.

We compare four basic situations regarding the effects of the same total amount of stressor: (1) homogeneous environment without dispersal, (2) homogeneous environment with dispersal, (3) heterogeneous environment without dispersal, and (4) heterogeneous environment with dispersal on the total population abundance at equilibrium (TRAPA). There are no losses of mortality due to the dispersal itself. Note that we use the same term for homogeneous environment with and without dispersal (cases 1 and 2) because dispersal does not alter TRAPA in the homogeneous environment (Zhang et al. 2017). We now define the four cases as $\text{TRAPA}_{\text{homogeneous}}$ (both case 1 and case 2), $\text{TRAPA}_{\text{heterogeneous,no dispersal}}$ (case 3), and $\text{TRAPA}_{\text{heterogeneous,dispersal}}$ (case 4). The objective of the analysis is to determine the ordering of these in terms of size for effects of stressor on each parameter.

Simulation Methods

We complement our experimental and analytical investigation with extensive simulations to explore a wider range of parameter space than is available with either our experimental system or mathematical techniques. In spatially homogeneous simulations, parameter values were identical in each patch. Spatial heterogeneity was introduced by allowing parameters (maximum growth rate [$r_{\max}$], yield [γ], and mortality rate of the consumer [m]) to deviate from homogeneity as described for the generic y above in "Mathematical Theory." Variation was always discrete, with two states. The mean of the two states corresponded to the value used in the spatially homogeneous simulation. For example, for variable $r_{\max}$ the spatially homogeneous value was $r_{\max} = 0.35$ in all patches, while in the spatially heterogeneous case patches alternated between $r_{\max} = 0.2$ and $r_{\max} = 0.5$. Parameters vary among patches in either a correlated or an anticorrelated fashion. Positively correlated parameters, such as $r_{\max}$ and γ, were established with the relationship $x_i = \alpha y_i$, where x and y denote the parameters, i denotes the patch, and α denotes a positive constant of proportionality; for negatively correlated parameters, $x_i = \alpha y_{i+1}$. Since variation alternates between adjacent patches, the negative correlation is generated by pairing the high value of one parameter with the low value of the other within a patch.

To imitate the experiment, the simulations assumed periodic replenishment of nutrient and stressor (see "Experimental Methods" below). We compared the relative relationships between $\text{TRAPA}_{\text{heterogeneous}}$ and $\text{TRAPA}_{\text{homogeneous}}$ across ranges of the nutrient input rate, N_{input}, and the dispersal rate, D. Simulations were iterated for sufficiently long to reach steady state. Spatially homogeneous and heterogeneous scenarios were implemented by modifying system parameters as described above in "Mathematical Theory." Simulations were performed in Matlab R2018b (Mathworks 2018).

Experimental Methods

Following Zhang et al. (2017), we conduct experiments using experimental metapopulations of the budding yeast (*Saccharomyces cerevisiae*; fig. 1). Yeast is a widely used experimental system that has the advantages of small size (5 μm), fast generation time (90 min), and ease of culturing. Therefore, using yeast allows us to establish a large number of replicate metapopulations in a very small space (eight replicate 12-subpopulation metapopulations in a single 4 × 6-inch 96-well microtiter plate), to accurately control nutrient and stressor environments, to accurately control population structure (e.g., dispersal pattern and rate), and to do all of this in a high-throughput setting over a large number of generations (10/day) in a short time period. In addition, yeasts and other fungi are important human pathogens that are widely treated with antibiotics, and the Centers for Disease Control and Prevention lists drug-resistant *Candida*, a yeast genus closely related to *Saccharomyces*, as a "serious threat" on its list of greatest antimicrobial resistance threats.

Strain and Culture Medium

We performed experiments with an auxotrophic, haploid (MATa) strain of the budding yeast (*S. cerevisiae*). This strain was constructed in the W303 background, with MATa can1-100 hml$\alpha\Delta$::BLE leu9Δ::KANMX6 trp2::NATMX4 (the strain was provided as a generous gift from M. Muller and A. Murray; Muller et al. 2014). This strain can synthesize all amino acids except tryptophan. The base growth medium consisted of 0.74 g/L complete synthetic medium minus tryptophan (Sunrise Science), 44.04 mg/L tryptophan, and 20 g/L dextrose. All reagents were added to the mixture and then autoclaved for sterilization. Medium was supplemented with the antiprokaryotic antibiotics tetracycline and ampicillin (which have no effect on yeast) to prevent bacterial contamination. Depending on the treatment, we included varying concentrations of the macrolide eukaryotic antibiotic cycloheximide as the yeast stressor. Cycloheximide binds eukaryotic ribosomes, inhibiting translation by interfering with translation elongation. The culture medium in all treatments was identical (uniform nutrient environment) except for potential differences in the average concentration or spatial pattern of cycloheximide. Cultures were propagated asexually.

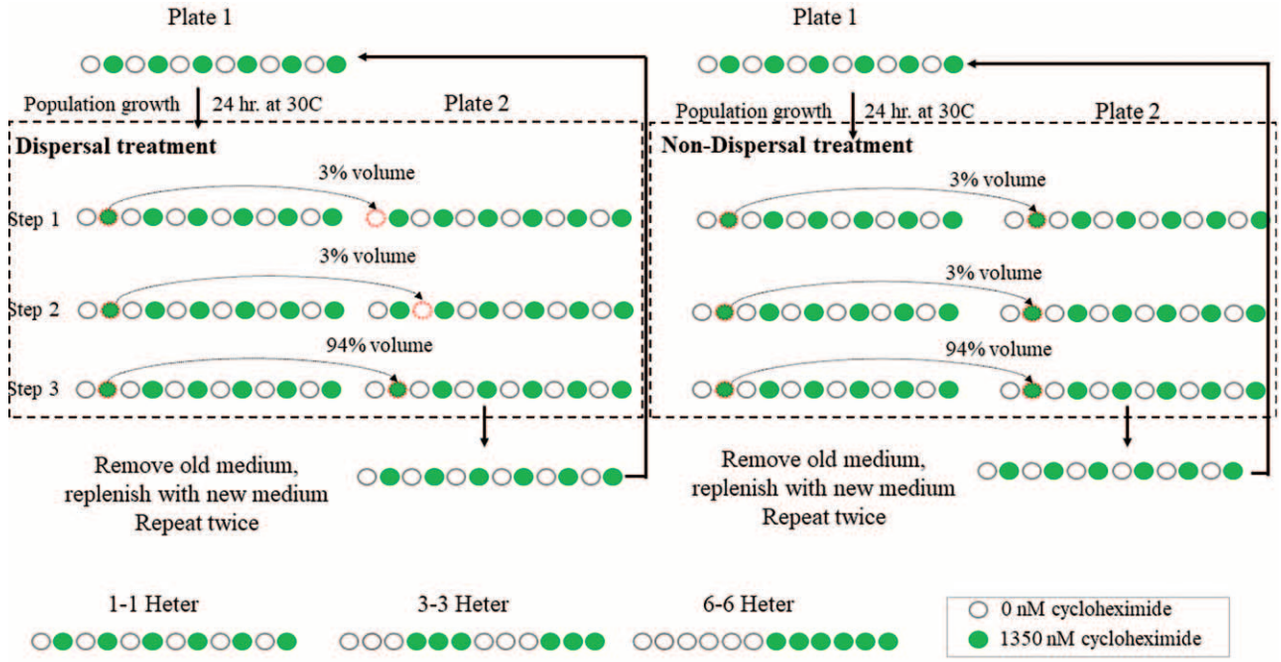

Figure 1: Schematic figure of the dispersal protocol. A metapopulation is composed of 12 discrete patches/wells arranged in a linear spatial array wherein dispersal occurs via random, bidirectional movement of a fraction of the population between nearest-neighbor patches, with reflecting (zero-flux) boundary conditions. Taking the 6% dispersal rate as an example, in the dispersal treatment 6% yeast volume was aspirated from each well in the original plate, and then 3% volume was dispensed to the adjacent well to the left as well as to the adjacent well to the right in the new plate; in the nondispersal treatment, 3% yeast volume was aspirated from each well in the original plate and then dispensed to the same well in an empty new plate twice. Last, in both treatments the remaining 94% yeast volume was dispensed to the same well in the new plate. After the dispersal process, old medium was removed and refilled twice with fresh medium. The new plate with fresh yeast medium was looped back to repeat the processes to reach the equilibrium point. White cells represent wells with 0 nM cycloheximide, and green ones represent wells with 1,350 nM cycloheximide. 1-1 Heter = alternating between 0 and 1,350 nM cycloheximide; 3-3 Heter = alternating between three wells of 0 and 1,350 nM cycloheximide; 6-6 Heter = alternating between six wells of 0 and 1,350 nM cycloheximide.

Establishment and Propagation of Spatial Populations

A single replicate population was established as one row of 12 wells in a round-bottom 96-microwell plate (Costar; see fig. 1). Each subpopulation (well) contained 124 μL of liquid growth medium, as described in the previous section, with some wells supplemented with cycloheximide according to treatment (see below).

Initial populations were established from a single overnight culture inoculated from freezer stock into 5 mL of YPD (20 g/L yeast extract, 10 g/L peptone, 20 g/L dextrose) and incubated at 30°C with constant agitation in a roller drum shaker. The saturated culture was washed three times with sterile water, and 124 μL of this culture was transferred into each well of a 96-well plate and then diluted by a factor of 2^{10} using a Biomek FXP liquid-handling robot.

Every 24 h, the 96-well plate was shaken at 1,350 rpm on a Titramax 1000 plate shaker to completely disperse the cell pellets. We then measured population density using a microplate photometer (Tecan Infinite M200 Pro) three times, taking the average of these three technical replicates to obtain the optical density at 660 nm (OD_{660}) of each well.

Next, each plate was subjected to either a dispersal or a nondispersal protocol, depending on treatment. Dispersal was implemented by taking a fraction of the total volume in each well and dispersing equal volumes to each of the two neighboring wells. As an example, consider a 6% dispersal rate. For the dispersal protocol, 3% volume was aspirated from each well in plate 1 and then dispersed to the adjacent position to the left of plate 2, which is a new empty plate, using the liquid-handling robot. Another 3% volume was dispersed into the adjacent position to the right. Last, the remaining volume in plate 1 was dispensed into plate 2 in the same position. For the nondispersal protocol, the three transfer steps were conducted exactly the same except that the total volume was dispersed to the same position from plate 1 to plate 2. Note also that the two perimeter columns of the plate (columns 1 and 12) received dispersed population from only one adjacent column (for more details, see

fig. 1). To avoid medium dispersal along with the yeast cells, after the dispersal process we washed cells twice by centrifuging plate 2 at 2,400 rpm for 5 min, removing supernatant and refilling with fresh medium using the liquid-handling robot. We repeated this twice. We then shook the plate on a plate shaker for at least 1 min to completely disperse the cell pellets and then incubated it unshaken at 30°C for 24 h. Consequently, both nutrients and toxicant were renewed in periodic pulses every 24 h. This passaging and dispersal procedure was repeated for 11 days, at which point the population densities for all treatments had approached an asymptote.

It is important to note that the experiment is necessarily slightly different from our chemostat model (eqq. [2]). Our experimental system imposes pulsed replenishment of resources and stressor, whereas our theory makes the standard assumption of continuous flow of resource and stressor. The theoretical assumption is necessary for analytical tractability, while the experimental setup is necessary for experimental tractability. Our simulations imitate the experiment, with periodic replenishment. As we will show in "Results," the qualitative match of theory, experiments, and simulation results indicates that the continuous flow assumption of the theory is a good approximation to the experimental conditions.

Experimental Treatments

Our experiment was a full factorial design consisting of three factors: dispersal rate (0% and 6%), average cycloheximide concentration (675 and 1,000 nM), and spatial pattern of cycloheximide (homogeneous, heterogeneous 1-1, heterogeneous 3-3, and heterogeneous 6-6). We also tested dispersal rates of 12% and 24% with the heterogeneous 1-1 configuration under both average cycloheximide concentrations (675 and 1,000 nM). Homogeneous treatments had a uniform concentration of cycloheximide in each of the 12 subpopulations. The heterogeneous 1-1 treatment alternated between one well without cycloheximide (0 nM) and one well with cycloheximide (1,350 or 2,000 nM; we use the heterogeneous environment with alternation between 0 and 1,350 nM cycloheximide as an example to demonstrate our experimental protocol in fig. 1); likewise, heterogeneous 3-3 (or 6-6) treatments alternated between three (or six) wells without cycloheximide and three (or six) wells with cycloheximide (see fig. 1). Each treatment was replicated four times.

Growth Parameter Estimation

Growth rate (r) follows the Monod equation, which depends on the available amount of essential growth resource (tryptophan) and specific growth parameters of r_{max}, K_S, and yield (Tilman 1982). The growth parameters r_{max} and K_S were estimated from the Monod equation generated from growth curve measurements at varying levels of tryptophan (0.734, 3.67, 7.34, 14.68, 29.36, 44.04, 58.73, 73.4, and 293.6 mg/L) and cycloheximide (0, 50, 200, 400, 675, 1,000, 1,350, and 2,000 nM) in all possible combinations, with three replicates for each combination. We used standard laboratory instruments (OD plate readers) for measuring growth curves in batch culture. A round-bottom 96-well plate with a factor of 2^{10} initial dilution was incubated in a Tecan Infinite M200 Pro plate reader at 30°C with constant orbital shaking at 280.8 rpm. Cell density was measured by OD_{660} every 15 min until the OD_{660} closely approached an asymptote (typically 24–72 h depending on the growth medium).

Each growth curve was fit to the standard logistic equation using custom fit in Matlab R2018b (Mathworks 2018) in order to estimate r (per capita growth rate when the population is close to zero) for each growth condition when the yeast abundance grows to equilibrium. We then used a Monod equation to fit the relationship between tryptophan concentrations and growth rate (r) to estimate r_{max} and K_S at a cycloheximide concentration between 0 and 675 nM. The Monod equation is $r = r_{max} \times [\text{tryptophan}]/(K_S + [\text{tryptophan}])$, where r_{max} is the asymptotic growth rate under infinite resources (refer to $r_{max,i}$ in eq. [2a]), [tryptophan] is the initial tryptophan concentration (refer to N_i in eq. [2a]), and K_S is the half-saturation coefficient (refer to K_S in eq. [2a]), defined as the value of [tryptophan] where $r = r_{max}/2$. Note that the estimation of r_{max} and K_S at higher cycloheximide concentrations (>675 nM) was not accurate enough because we had very low yeast growth at higher cycloheximide concentrations so that the accuracy of curve fitting was affected. Therefore, at higher cycloheximide concentrations (>675 nM) r_{max} was estimated as the r at the tryptophan concentration where yeast growth was not further limited by this resource. In this case, we selected the tryptophan concentration of 293.6 mg/L, whereas K_S could still not be estimated.

We estimated yield as $\gamma = \text{final } OD_{600}/[\text{tryptophan}]$, where [tryptophan] is the tryptophan concentration of the growth medium before inoculation with yeast under the tryptophan conditions of our spatial population experiments (44.04 mg/L) for the following concentrations of cycloheximide: 0, 50, 200, 400, 675, 1,000, 1,350, and 2,000 nM.

To estimate the density-independent and density-dependent death rates (m and g, respectively), we performed a live/dead cell stain (LIVE/DEAD FungaLight Yeast Viability Kit; Molecular Probes) of cultures exposed to different levels of cycloheximide (0, 337.5, 675, 1,350, and 2,000 nM) and different initial cell densities (OD_{660}; 0.2, 0.5, 0.8, 1.1,

and 1.4) in all possible combinations with three replicates of each treatment. We propagated cultures using the nondispersal protocol described above and then measured the fraction of live and dead cells in each culture at two time points, 0 and 91 h, to determine the death rate.

The live/dead cell stain was performed as follows. At the time of staining, 100 μL was sampled from each replicate culture and subdivided into two subsamples. Then 40 μL of sample was used as a dead cell control, which was prepared by adding 100 μL of 70% ethanol and incubating at room temperature for 1 h. The remaining 60 μL of the sample served as the experimental sample. Then all samples were washed twice with 100 μL of cold phosphate-buffered saline (PBS) without tween and resuspended in 100 μL of PBS. Cell density (OD_{660}) was measured using a Tecan Infinite M200 Pro plate reader and then diluted to a cell density of $\sim 0.6 \times 10^6$ with PBS. Then 55 μL of diluted samples was mixed with 0.55 μL of 1/10 diluted propidium iodide and incubated at 30°C for 30 min, and the fluorescence of each sample was measured with a BD Accuri C6 flow cytometer. Since propidium iodide only stains yeast cells with damaged membranes, dead cells fluoresce red while live cells are dark. The death rate was estimated using the following equation:

$$\text{death rate (\%/15 min)} = \frac{\text{death (\% at 91 h)} - \text{death (\% at 0 h)}}{91 \text{ h} \times 4}.$$

We used a linear function to fit the relationship between measured death rate (1% loss every 15 min) and initial cell density (OD_{660}) at each cycloheximide concentration for the estimated density-independent death rate, m, and the density-dependent death rate, g. The linear function is measured death rate $= g \times [\text{initial cell density } (OD_{660})] + m$. Note that we chose this unit of death rate to match the unit of growth rate we used in the earlier part of the article.

Data Analysis

The total realized asymptotic population (TRAPA) achieved was calculated as the sum of OD_{660} over all of its subpopulations (i.e., 2–11 wells). The combined effect of distribution (heterogeneous vs. homogeneous) and dispersal rate (0%, 6%, 12%, and 24%) on TRAPA was quantified by analysis of variance (ANOVA). The ANOVA was implemented through the JMP statistical program (Sall 2012). Its assumptions of homoscedasticity and normality of the residuals were satisfied by checking the residual plot by the predicted values and the Shapiro-Wilk W-test ($P > .05$), respectively. The assumption about the zero expectation of the residuals was shown to be satisfied by comparing the residual expectation with zero in the one-sample t-test ($P = .5$).

Results

Theoretical Results

Both mathematical analyses and simulations were performed with models 1 and 2 (eqq. [2a], [2b]). We show only the results of simulations of model 2, the chemostat model of consumer and resource; for more details, see the supplemental PDF. Note that mathematical analyses of models 1 and 2 could be performed only for the limiting cases $0 < D \ll 1$ and $D \to \infty$, and they were also limited here to source-source conditions for the two patches.

The simulations of model 2, depicted as heat maps (fig. 2), are comprehensive results of the differences between the total realized asymptotic populations achieved (TRAPAs) for each of the three parameters r_{max}, γ, and m, with these parameters being either homogeneously ($TRAPA_{homogeneous}$) or heterogeneously ($TRAPA_{heterogeneous}$) distributed across two patches (reflecting distribution of the stressor), where the populations are dispersing symmetrically in each case. Remarkably, the simplest simulation outcomes also happen to coincide with the most biologically realistic cases, at least when the stressor acts like an antibiotic by either increasing mortality, m, or inhibiting growth, r_{max}, and/or yield, γ.

Along the black dashed-dotted diagonal line when the two parameters vary simultaneously, we found that when stressors decrease r_{max} or γ (panels 1 and 5), $TRAPA_{heterogeneous} > TRAPA_{homogeneous}$, which was opposite to a decrease in m (panel 9) that lead to $TRAPA_{heterogeneous} > TRAPA_{homogeneous}$. Above the diagonal line, when the two parameters are positively correlated, we found that a homogeneous distribution of stressor caused the lowest TRAPA only when r_{max} and γ are positively correlated (panel 2). In addition, if r_{max} and m or m and γ are positively correlated, $TRAPA_{heterogeneous} > TRAPA_{homogeneous}$ (panels 3 and 6). Below the diagonal line, when the two parameters are negatively correlated, a homogeneous environment has a larger TRAPA only when r_{max} and γ are negatively correlated (panel 4), which was opposite to panel 2. Last, when r_{max} and m or m and γ are negatively correlated, $TRAPA_{heterogeneous} > TRAPA_{homogeneous}$ (panels 7 and 8), which were also opposite to panels 3 and 6.

The mathematical results with the limiting case $0 < D \ll 1$ can be compared with the results in figure 2. For model 1 for $0 < D \ll 1$, there was no difference between heterogeneity and homogeneity for r_{max}. For γ, results agreed with panel 5 in figure 2, $TRAPA_{heterogeneous} < TRAPA_{homogeneous}$, which means that if this parameter were decreased, the homogeneous distribution would lead to the lowest TRAPA. For parameter m, consistent with panel 9 in figure 2, the population size for the heterogeneous parameter m was

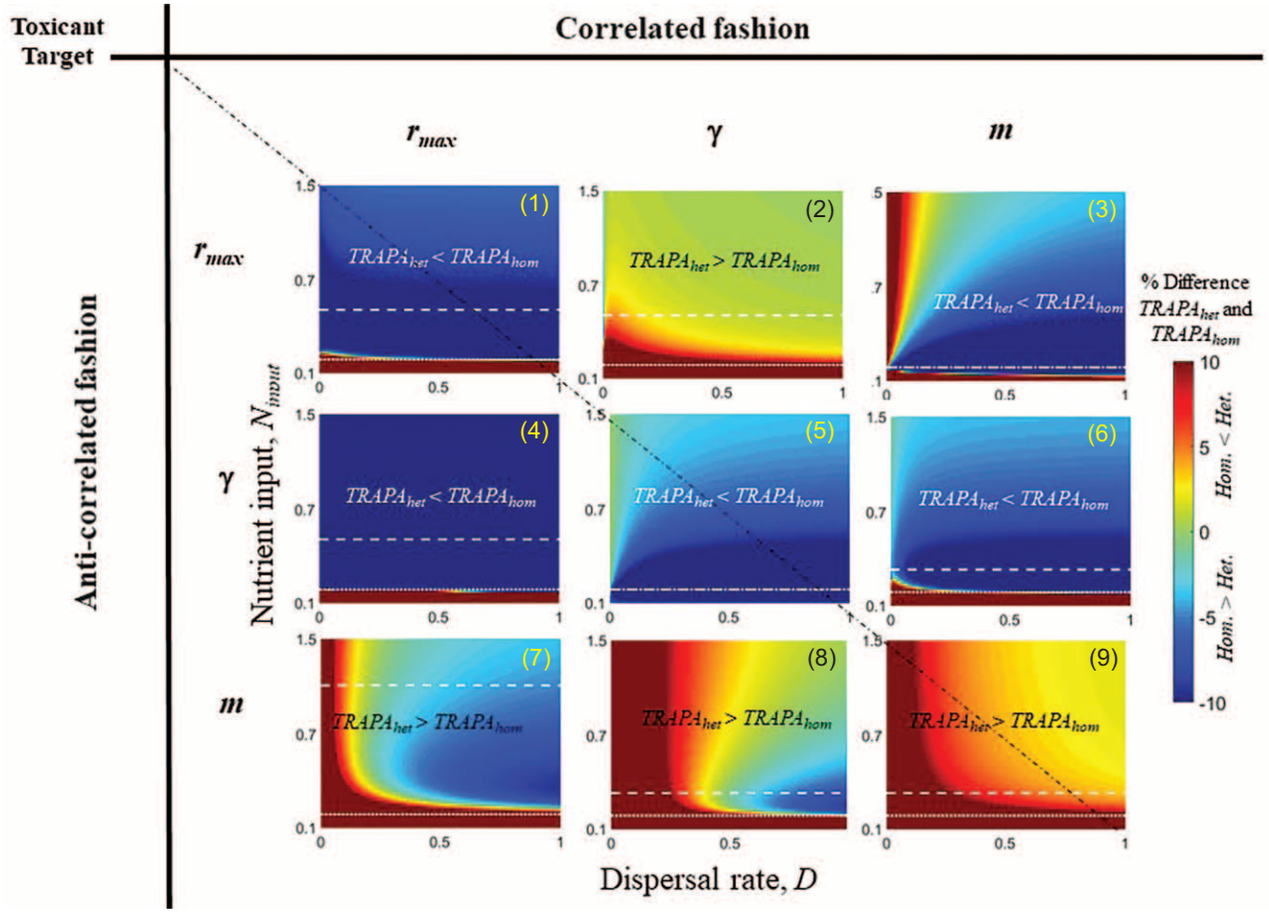

Figure 2: Simulation results reveal the complex interaction between a stressor's effect on different components of fitness and heterogeneity on total realized asymptotic population abundance (TRAPA; total population abundance at equilibrium). The columns and rows of the matrix are the three parameters: maximum growth rate (r_{max}), yield (γ), and mortality rate of the consumer (m). Spatial heterogeneity was introduced by allowing one, two, or three parameters to vary among patches in either a correlated or an anticorrelated fashion. The three subplots along the black dashed-dotted diagonal line represent scenarios where only one parameter is affected/changed, the three subplots above the diagonal line represent scenarios where the two parameters are positively correlated, and the three subplots below the diagonal line represent scenarios where the two parameters are negatively correlated. The vertical axis of each heat map varies the nutrient input rate, N_{input}, while the horizontal axis varies the dispersal rate (D). For nutrient values above the dashed horizontal line in each subplot, all patches support a viable population (source-source); that is, each can maintain a steady-state population on its own. Between the dashed and dotted horizontal lines, one of the patches in the heterogeneous case is a sink, while the other is a source (source-sink); that is, one patch type supports zero individuals at steady state in the absence of dispersal, as would occur if the stressor added to a patch was high enough to completely suppress population growth. Below the dotted horizontal line, the homogeneous population is inviable, while the "high" patch in the heterogeneous case is viable. The color of the heat maps quantifies the relative degree to which a heterogeneous population ("Het") differs from a homogeneous population ("Hom"). Warm colors indicate that $\text{TRAPA}_{\text{heterogeneous}} > \text{TRAPA}_{\text{homogeneous}}$, while cool colors indicate the opposite inequality.

always greater than that of the homogeneous population. In model 2 for the limiting case $0 < D \ll 1$, for heterogeneity of r_{max}, $\text{TRAPA}_{\text{heterogeneous}} < \text{TRAPA}_{\text{homogeneous}}$, in agreement with panel 1. For yield, γ, there was no difference in whether γ was heterogeneous or homogeneous. For parameter m, in agreement with panel 9, $\text{TRAPA}_{\text{heterogeneous}} \geq \text{TRAPA}_{\text{homogeneous}}$. In addition, consistent with the simulation results, when r and γ were positively correlated, then $\text{TRAPA}_{\text{homogeneous}} < \text{TRAPA}_{\text{heterogeneous}}$ as long as the population is dispersing in the heterogeneous case. Therefore, the analytic results of model 1 are generally similar to those of model 2 and to those of the simulation results of figure 2.

Experimental Results

Effects of Cycloheximide on Yeast Growth Parameters. We estimated the responses of all growth parameters in equations (2) to cycloheximide stress. Maximum growth

rate (r_{max}) and yield (γ) had a positively correlated response to cycloheximide exposure ($\gamma = 0.05 \times r_{max} + 0.02$; $R^2 = 0.78$; fig. 3*F*), with both parameters decreasing as a function of cycloheximide concentration (fig. 3*A*, 3*C*). Likewise, the half-saturation parameter, K_S, increased with increasing cycloheximide dose, indicating a reduction in nutrient use efficiency, as more nutrients were required to achieve a given growth rate as cycloheximide levels increased (fig. 3*B*). Finally, only at a high cycloheximide concentration (2,000 nM) did both density-independent death rate (m) and density-dependent death rate (g) show a significant difference from lower cycloheximide concentrations ($P < .001$ and $P = .001$, respectively; fig. 3*D*, 3*E*).

Effect of Dispersal and Heterogeneity on TRAPA. Consistent with our theoretical predictions that a heterogeneous distribution of stressor causes higher TRAPA if r and γ are positively correlated, we measured a significantly larger TRAPA in treatments with spatial heterogeneity and dispersal. With the lower average cycloheximide concentration (675 nM), TRAPA was significantly higher with dispersal (6%) than with nondispersal (0%; $P = .0038$; fig. 4*A*) in the heterogeneous 1-1 environment. There was no statistically significant difference in TRAPA among nonzero dispersal levels (6%, 12%, and 24%; $P > .05$). In the homogeneous environment, there was no significant difference in TRAPA between dispersal (6%) and nondispersal (0%; $P = .1127$), as predicted (fig. 4*A*). Importantly, TRAPA in the homogenous environment, with or without dispersal, was always significantly lower than TRAPA in the heterogeneous environment with dispersal ($P < .0001$).

In the high average cycloheximide treatment (1,000 nM), the heterogeneous, nondispersal treatment had significantly lower TRAPA than any other treatment ($P < .0001$; fig. 4*B*). In addition, a higher dispersal rate, especially intermediate dispersal (12%), resulted in a significantly higher TRAPA than did 6% in the heterogeneous environment ($P = .0035$). Consistently, TRAPA in the heterogeneous environment with dispersal was significantly higher than TRAPA in the homogeneous environment with or without dispersal ($P < .0001$). That TRAPA was smaller in the heterogeneous treatment without dispersal than with dispersal can be explained by the model prediction that if r and γ are positively correlated, heterogeneous environments support larger TRAPA when species disperse (figs. S4.4, S5.2 in the supplemental PDF).

Furthermore, the effect of the spatial pattern of heterogeneity on TRAPA followed a predictable pattern. In the lower average cycloheximide treatment (675 nM), TRAPA with dispersal was significantly larger than that with nondispersal only in the heterogeneous 1-1 and 3-3 treatments ($P = .0247$ and $P = .0182$, respectively) but not in the 6-6 treatment ($P = .2564$), indicating the large spatial clusters of habitat diminish the effect of heterogeneity on TRAPA (fig. 4*C*). However, in the higher average cycloheximide treatment (1,000 nM), all three spatial designs resulted in significantly larger TRAPA with dispersal than without dispersal (1-1: $P < .0001$; 3-3: $P < .0001$; 6-6: $P = .0022$) but with a larger effect in the heterogeneous 1-1 and 3-3 treatments than in the heterogeneous 6-6 treatment (fig. 4*D*). These results indicate that the population-level effect of the stressor depends not only on the average level of heterogeneity of the stressor but also on the spatial pattern of heterogeneity.

A summary of theoretical proofs of the effect of antibiotic heterogeneity with dispersal on TRAPA is shown in table 1.

Discussion

Selection pressures, including resources, predators/grazers, and stressors, are typically distributed unevenly over the landscape, creating environmental heterogeneity. There is growing interest in how the spatial distribution of selection pressures determines the size of metapopulations (Holt et al. 2003; Lou 2006; Zhang et al. 2015, 2017). However, we are unaware of any studies examining how the spatial heterogeneity of a stressor (i.e., a factor with a negative effect) affects metapopulation size. Therefore, here we first derived new mathematical results. Simulations demonstrate that the impact of stressor heterogeneity on total equilibrium population size depends sensitively on the interaction between dispersal rate and the physiological effect of the stressor, that is, on whether the stressor alters the maximum population growth rate, r_{max}; the nutrient assimilation efficiency (or yield), γ; or the density-independent and/or density-dependent mortality rates m and g (fig. 3). For many possible stressor physiological impacts, the effect of a stressor on total population size may change signs as either heterogeneity or the dispersal rate changes (fig. 4), placing limitations on the ability to predict outcomes in natural populations without precise data. Remarkably, though, while the complexity of such a system appears bewildering at first, we were able to find general mathematical proofs for two cases of wide relevance. Specifically, we proved that stressors that either increase the death rate (e.g., bactericidal antibiotics) or negatively impact both the growth rate and the yield (e.g., some bacteriostatic antibiotics) will always have the greatest impact on a randomly dispersing population when these are homogeneously distributed over space. That is, for these types of stressors, metapopulation size is minimized with a homogeneous stressor distribution. We then validated our theoretical results by using spatially structured laboratory populations of budding yeast using an experimental setup that has been rigorously validated as an accurate experimental model of spatial population

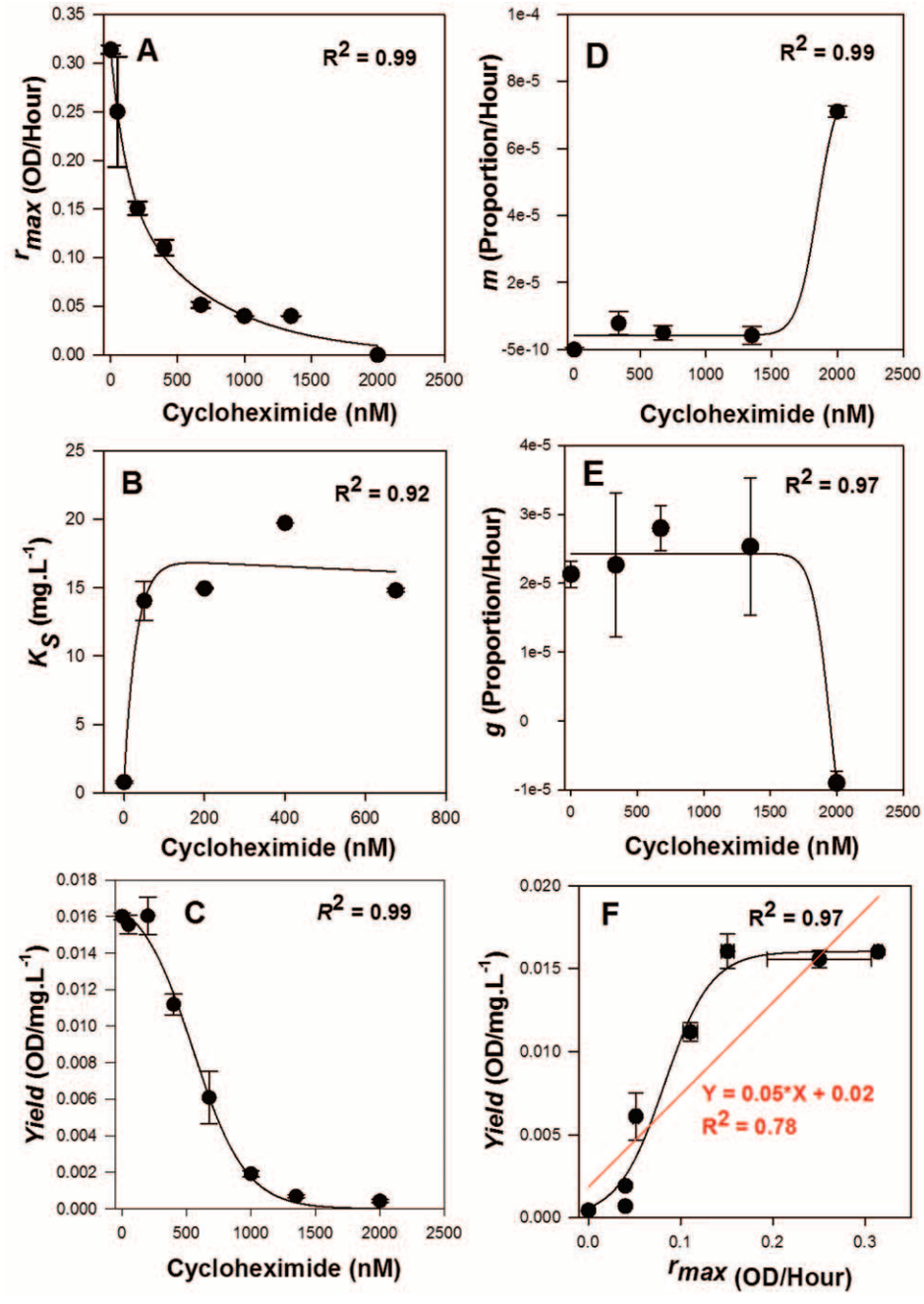

Figure 3: Effect of a stressor on population growth parameters: *A*, maximum growth rate (r_{max}); *B*, half-saturation coefficient (K_s); *C*, yield (γ); *D*, density-independent death rate (m); *E*, density-dependent death rate (g); *F*, correlation between maximum growth rate (r_{max}) and yield (γ) response to stressor (cycloheximide) exposure. *A* and *B* were fitted by a biexponential function, and *C*–*F* were fitted by a logistic function (black line). *F* was also fitted by a linear regression (red line). OD = optical density.

dynamics. We first determined that the antibiotic cycloheximide increases the yeast death rate but reduces the growth rate and yield. Then, consistent with our theoretical predictions, we experimentally observed that a spatially homogeneous application of stressor had the greatest impact on a metapopulation, even under conditions where the stressor had negligible effects on mortality.

The mathematical and empirical results demonstrate that the same amount of stressors with different spatial distributions resulted in different effects on the metapopulation.

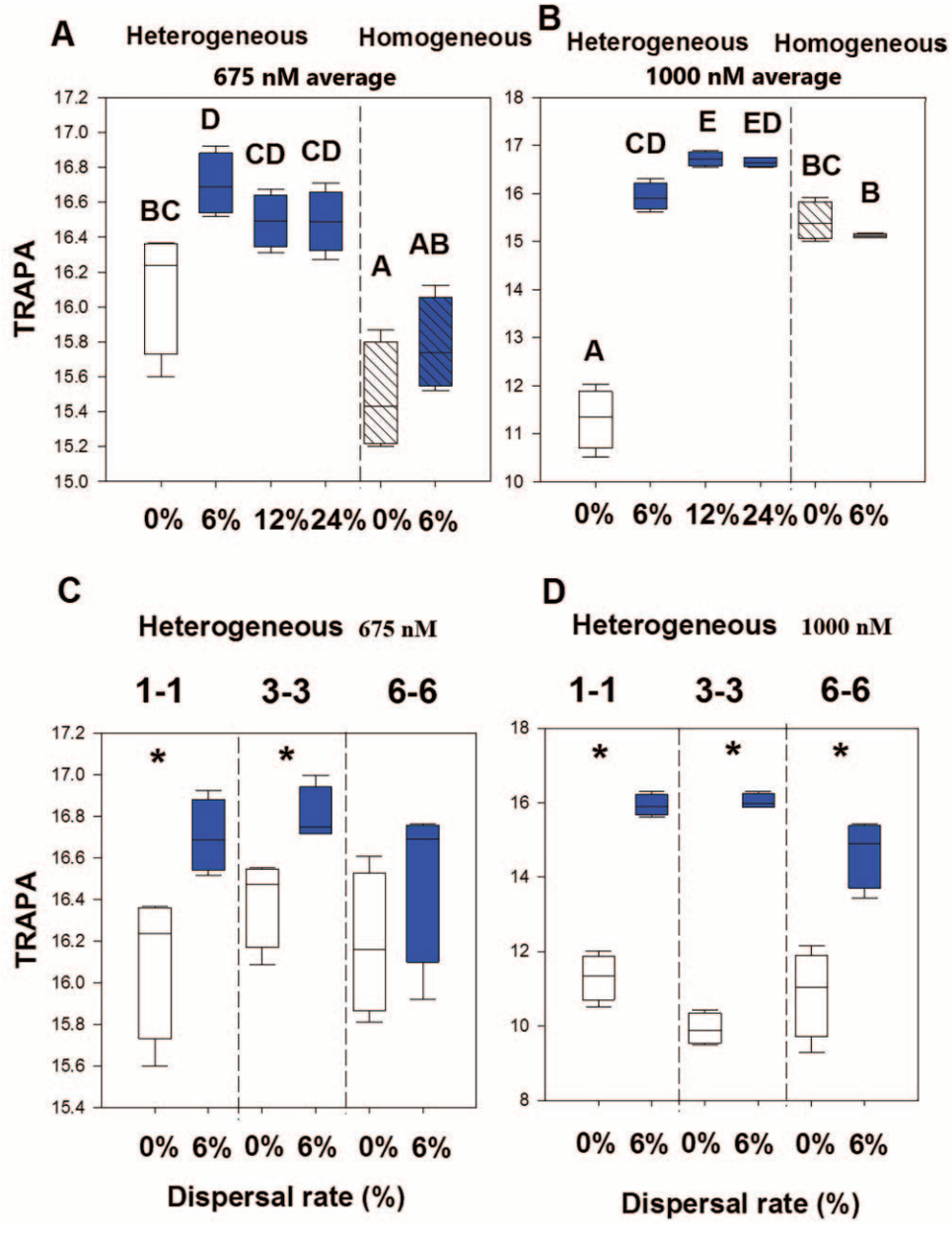

Figure 4: Experimental results showing that connectivity and stressor heterogeneity increase total population size. Shown are the total realized asymptotic population abundance (TRAPA) with four replicates with different dispersal rates in heterogeneous and homogeneous environments with an average cycloheximide concentration of 675 nM (*A*), heterogeneous and homogeneous environments with an average cycloheximide concentration of 1,000 nM (*B*), a heterogeneous environment with three pattern designs and an average cycloheximide concentration of 675 nM (*C*), and a heterogeneous environment with three pattern designs and an average cycloheximide concentration of 1,000 nM (*D*). Different letters in *A* and *B* indicate significant differences ($P < .05$) among different treatments, and asterisks in *C* and *D* indicate that there was significantly higher TRAPA with dispersal ($P < .05$).

That a homogeneous distribution of a stressor leads to a smaller metapopulation than any heterogeneous distribution has a straightforward intuitive explanation. In an environment with a heterogeneously distributed stressor, low-stress patches act as sources that overfill neighboring high-stress patches with dispersal. The dispersal into high-stress patches from low-stress patches allows high-stress patches to exceed their local stress-influenced carrying capacity despite

Table 1: Summary of theoretical proofs of the effect of antibiotic heterogeneity with dispersal on total realized asymptotic population abundance (TRAPA; total population abundance at equilibrium), according to the parameters in equations (2)

Parameter	Symbol	Effect of antibiotic heterogeneity with dispersal on TRAPA
Mortality (density independent)	m	Positive ($\geq$)
Mortality (density dependent)	g	Positive ($\geq$)
Yield	γ	Negative ($\leq$)
Asymptotic growth rate	r_{max}	Negative ($\leq$)
Negatively correlated m and γ	m and γ	Positive ($\geq$)
Positively correlated r_{max} and γ	r_{max} and γ	Positive ($\geq$)

Note: Positive effect means $TRAPA_{heterogeneous} > TRAPA_{homogeneous}$, and negative effect means $TRAPA_{heterogeneous} < TRAPA_{homogeneous}$.

high loss rates on the high-stress patches. The gains in total carrying capacity at the metapopulation level, then, come from dispersal from low-stress patches overfilling high-stress patches. This compensatory effect in earlier research is described in Harrington et al. (2005). Note that for this effect to occur generally, the stressor must alter both the growth rate and the local carrying capacity. This condition is satisfied when the stressor alters both the growth rate and yield or just the death rate, consistent with our theoretical results. On the other hand, with a uniform distribution of stressor, there is no opportunity for dispersal to overfill local patches, since all patches have the same local stress-determined carrying capacity. Because of the causal effect of stressor heterogeneity on total population size, our work supports earlier research showing the importance of considering habitat pattern in species conservation (Fahrig 2002).

While the spatial distribution of a stressor alters total population size, the extent of this effect depends on dispersal. We observed that when the stressor amount is high and heterogeneously distributed, an intermediate dispersal rate appeared to maintain the largest metapopulation, which agrees with previous studies (Santamaria 2002; Zhang et al. 2015). This positive effect demonstrates that dispersal may be a factor that can maintain high populations when environmental conditions are declining (Hansson 1991; Clobert et al. 2009; Chapman et al. 2012), through subsidies to less productive patches by more productive patches (Kotze and O'Hara 2003; Aviron et al. 2007).

As noted in the introduction, our work is related to a large body of theory on dispersing populations in heterogeneous environments (Holt 1985; Freedman et al. 1987; Law et al. 2003; Lou 2006; Herbener et al. 2012; DeAngelis et al. 2020). As described in supplement 1, some theoretical work on two-patch logistic populations linked by diffusion appeared to suggest that the total size of the equilibrium metapopulation with dispersal among the heterogeneous patches could exceed the sum of carrying capacities when the carrying capacities were distributed homogeneously among the patches. It was shown mathematically using a consumer-resource model in He et al. (2019) and Wang and DeAngelis (2019) that a homogeneously distributed resource input always resulted in a total size (TRAPA) of a diffusing metapopulation that is equal to or larger than the metapopulation size when the same amount of resource input is heterogeneously distributed, which was confirmed experimentally (Zhang et al. 2017).

What we have shown here is the converse of the above-described situation, where now instead of a resource, a stressor having a negative effect on a population is distributed either homogeneously or heterogeneously. In this case, the homogeneous distribution mathematically leads to a lower metapopulation size (TRAPA) than any heterogeneous distribution when the mortality parameters or a positively correlated combination of yield and maximum population growth rate are considered. Therefore, we are now able to conclude that positive and negative environmental factors interact with habitat heterogeneity to generate qualitatively different outcomes at the metapopulation level.

We are aware that the settings used in the model and experiment are quite simple compared with real natural systems, but the conclusions that we gained from this work can have broad implications in ecology. Our work advances our earlier understanding of the effect of stressors on populations from experiments that were mostly performed in homogeneous (environmentally uniform), nonspatial (well-mixed) laboratory containers (Sibly et al. 2000; Liu et al. 2009) or at field sites under constant treatments (e.g., CO_2, warming, and drought; Sheik et al. 2011; Morrow et al. 2015). Therefore, future fieldwork should consider the heterogeneous distribution of stressors across the landscape (Joint et al. 2011) and look at the effect of stressors at the metapopulation level. In addition, this study gives some hints toward solving a central problem in determining how to prioritize treatment areas for the purpose of disease vectors and pathogen control. Specifically, our results suggest that equalizing the treatment level in different regions might be the most efficient strategy for minimizing the size of pest species (Giljohann et al. 2011; Arroyo-Esquivel et al. 2019). This finding can help field ecologists and managers identify the optimal management strategy that maximizes effectiveness given limited budgets and resources. Last, since dispersal increases metapopulation abundance

in a heterogeneous stressful environment, preventing invasive species from dispersing to new areas and creating dispersal pathway barriers might be another efficient solution for biological invasion control (Wilson et al. 2009). In general, our work here indicates that the effect of stressors on natural populations requires a detailed understanding of a population's dispersal structure, the degree of heterogeneity of a stressor over the population's range, and the mode of action of the stressor on individuals in the population.

Acknowledgments

We thank A. Murray and M. Mueller for providing strains. The editors and two anonymous reviewers provided insightful comments on the manuscript. This work was supported by the University of California, Davis, Chancellor's Postdoc Fellowship program (to B.Z.), the William H. Evoy Graduate Research and Savage Graduate Research Support Fund (to A.K.), and the National Science Foundation and the National Natural Science Foundation of China (to W.-M.N.). D.L.D. was supported by the Greater Everglades Priority Ecosystem Science program. Any use of trade, firm, or product names is for descriptive purposes only and does not imply endorsement by the US government.

Statement of Authorship

B.Z. and J.D.V.D. designed the research and experiments. B.Z., A.K., and S.X. conducted the experiment and collected data. L.Z. analyzed the data. D.L.D., W.-M.N., and Y.W. contributed to the mathematical analysis and proof. D.V.D. performed the simulations. B.Z., D.L.D., and J.D.V.D. wrote the first draft. All authors contributed to revisions of the manuscript.

Data and Code Availability

Laboratory data and Matlab code for simulations are available in the Dryad Digital Repository (https://doi.org/10.25338/B8090K; Zhang 2020).

Literature Cited

Andow, D. P. K., S. Levin, and A. Okubo. 1993. Spread of invading organisms: patterns of spread. Wiley, New York.

Arditi, R., C. Lobry, and T. Sari. 2015. Is dispersal always beneficial to carrying capacity? new insights from the multi-patch logistic equation. Theoretical Population Biology 106:45–59.

Arroyo-Esquivel, J., F. Sanchez, and L. A. Barboza. 2019. Infection model for analyzing biological control of coffee rust using bacterial anti-fungal compounds. Mathematical Biosciences 307:13–24.

Aviron, S., P. Kindlmann, and F. Burel. 2007. Conservation of butterfly populations in dynamic landscapes: the role of farming practices and landscape mosaic. Ecological Modelling 205:135–145.

Bond-Lamberty, B., A. V. Rocha, K. Calvin, B. Holmes, C. K. Wang, and M. L. Goulden. 2014. Disturbance legacies and climate jointly drive tree growth and mortality in an intensively studied boreal forest. Global Change Biology 20:216–227.

Chapman, J. W., J. R. Bell, L. E. Burgin, D. R. Reynolds, L. B. Pettersson, J. K. Hill, M. B. Bonsall, et al. 2012. Seasonal migration to high latitudes results in major reproductive benefits in an insect. Proceedings of the National Academy of Sciences of the USA 109:14924–14929.

Clobert, J., J. F. Le Galliard, J. Cote, S. Meylan, and M. Massot. 2009. Informed dispersal, heterogeneity in animal dispersal syndromes and the dynamics of spatially structured populations. Ecology Letters 12:197–209.

DeAngelis, D. L., W. M. Ni, and B. Zhang. 2016. Dispersal and spatial heterogeneity: single species. Journal of Mathematical Biology 72:239–254.

DeAngelis, D. L., B. Zhang, W.-M. Ni, and Y. Wang. 2020. Carrying capacity of a population diffusing in a heterogeneous environment. Mathematics 8:49.

Fahrig, L. 2002. Effect of habitat fragmentation on the extinction threshold: a synthesis. Ecological Applications 12:346–353.

Ferguson, N. M., Z. M. Cucunuba, I. Dorigatti, G. L. Nedjati-Gilani, C. A. Donnelly, M. G. Basanez, P. Nouvellet, et al. 2016. Countering the Zika epidemic in Latin America. Science 353:353–354.

Freedman, H. I., J. W. H. So, and P. Waltman. 1987. Predator influence on the growth of a population with 3 genotypes. III. Persistence and extinction. Journal of Mathematical Analysis and Applications 128:287–304.

Fritsch, C., P. Giraudoux, M. Coeurdassier, F. Douay, F. Raoul, C. Pruyot, C. Waterlot, et al. 2010. Spatial distribution of metals in smelter-impacted soils of woody habitats: influence of landscape and soil properties, and risk for wildlife. Chemosphere 81:141–155.

Gandhi, S. R., E. A. Yurtsev, K. S. Korolev, and J. Gore. 2016. Range expansions transition from pulled to pushed waves as growth becomes more cooperative in an experimental microbial population. Proceedings of the National Academy of Sciences of the USA 113:6922–6927.

Genin, A., S. Majumder, S. Sankaran, F. D. Schneider, A. Danet, M. Berdugo, V. Guttal, et al. 2018. Spatially heterogeneous stressors can alter the performance of indicators of regime shifts. Ecological Indicators 94:520–533.

Giljohann, K. M., C. E. Hauser, N. S. G. Williams, and J. L. Moore. 2011. Optimizing invasive species control across space: willow invasion management in the Australian Alps. Journal of Applied Ecology 48:1286–1294.

Ha, C. V., M. A. Leyva-Gonzalez, Y. Osakabe, U. T. Tran, R. Nishiyama, Y. Watanabe, M. Tanaka, et al. 2014. Positive regulatory role of strigolactone in plant responses to drought and salt stress. Proceedings of the National Academy of Sciences of the USA 111:851–856.

Hansson, L. 1991. Dispersal and connectivity in metapopulations. Biological Journal of the Linnean Society 42:89–103.

Harrington, L. C., T. W. Scott, K. Lerdthusnee, R. C. Coleman, A. Costero, G. G. Clark, J. J. Jones, et al. 2005. Dispersal of the

dengue vector *Aedes aegypti* within and between rural communities. American Journal of Tropical Medicine and Hygiene 72:209–220.

Hastings, A., K. Cuddington, K. F. Davies, C. J. Dugaw, S. Elmendorf, A. Freestone, S. Harrison, et al. 2005. The spatial spread of invasions: new developments in theory and evidence. Ecology Letters 8:91–101.

He, X. Q., K. Y. Lam, Y. Lou, and W. M. Ni. 2019. Dynamics of a consumer-resource reaction-diffusion model: homogeneous versus heterogeneous environments. Journal of Mathematical Biology 78:1605–1636.

Hendriks, A. J., J. L. M. Maas-Diepeveen, E. H. W. Heugens, and N. M. Van Straalen. 2005. Meta-analysis of intrinsic rates of increase and carrying capacity of populations affected by toxic and other stressors. Environmental Toxicology and Chemistry 24:2267–2277.

Herbener, K. W., S. J. Tavener, and N. T. Hobbs. 2012. The distinct effects of habitat fragmentation on population size. Theoretical Ecology 5:73–82.

Holt, R. D. 1985. Population dynamics in two-patch environments: some anomalous consequences of an optimal habitat distribution. Theoretical Population Biology 28:181–208.

Holt, R. D., R. Gomulkiewicz, and M. Barfield. 2003. The phenomenology of niche evolution via quantitative traits in a "black-hole" sink. Proceedings of the Royal Society B 270:215–224.

Hunt, J. W., B. S. Anderson, B. M. Phillips, R. S. Tjeerdema, N. Richard, V. Connor, K. Worcester, et al. 2006. Spatial relationships between water quality and pesticide application rates in agricultural watersheds. Environmental Monitoring and Assessment 121:245–262.

Joint, I., S. C. Doney, and D. M. Karl. 2011. Will ocean acidification affect marine microbes? ISME Journal 5:1–7.

Kimura, M., and G. H. Weiss. 1964. The stepping stone model of population structure and the decrease of genetic correlation with distance. Genetics 49:561.

Konopka, A. 2009. What is microbial community ecology? ISME Journal 3:1223–1230.

Kot, M., M. A. Lewis, and P. van den Driessche. 1996. Dispersal data and the spread of invading organisms. Ecology 77:2027–2042.

Kotze, D. J., and R. B. O'Hara. 2003. Species decline—but why? explanations of carabid beetle (Coleoptera, Carabidae) declines in Europe. Oecologia 135:138–148.

Law, R., D. J. Murrell, and U. Dieckmann. 2003. Population growth in space and time: spatial logistic equations. Ecology 84:252–262.

Lefebvre, K. A., C. L. Powell, M. Busman, C. J. Doucette, P. D. R. Moeller, J. B. Sliver, P. E. Miller, et al. 1999. Detection of domoic acid in northern anchovies and California sea lions associated with an unusual mortality event. Natural Toxins 7:85–92.

Levins, R. 1968. Evolution in changing environments: some theoretical explorations. Princeton University Press, Princeton, NJ.

Liu, F., G. G. Ying, R. Tao, J.-L. Zhao, J. F. Yang, and L. F. Zhao. 2009. Effects of six selected antibiotics on plant growth and soil microbial and enzymatic activities. Environmental Pollution 157:1636–1642.

Lou, Y. 2006. On the effects of migration and spatial heterogeneity on single and multiple species. Journal of Differential Equations 223:400–426.

MacArthur, R. H. 1972. Geographical ecology. Harper & Row, New York.

Mann, M. E., R. S. Bradley, and M. K. Hughes. 1998. Global-scale temperature patterns and climate forcing over the past six centuries. Nature 392:779–787.

Mathworks. 2018. Matlab and statistics toolbox release. Mathworks, Natick, MA.

Morrow, K. M., D. G. Bourne, C. Humphrey, E. S. Botte, P. Laffy, J. Zaneveld, S. Uthicke, et al. 2015. Natural volcanic CO_2 seeps reveal future trajectories for host-microbial associations in corals and sponges. ISME Journal 9:894–908.

Muller, M. J. I., B. I. Neugeboren, D. R. Nelson, and A. W. Murray. 2014. Genetic drift opposes mutualism during spatial population expansion. Proceedings of the National Academy of Sciences of the USA 111:1037–1042.

Reiners, W. A., and K. L. Driese. 2001. The propagation of ecological influences through heterogeneous environmental space. Bioscience 51:939–950.

Ruiz-Herrera, A., and P. J. Torres. 2018. Effects of diffusion on total biomass in simple metacommunities. Journal of Theoretical Biology 447:12–24.

Sall, J., A. Lehman, M. L. Stephens, and L. Creighton. 2012. JMP start statistics: a guide to statistics and data analysis using JMP. SAS Institute, Cary, NC.

Santamaria, L. 2002. Why are most aquatic plants widely distributed? dispersal, clonal growth and small-scale heterogeneity in a stressful environment. Acta Oecologica 23:137–154.

Sen Datta, M., K. S. Korolev, I. Cvijovic, C. Dudley, and J. Gore. 2013. Range expansion promotes cooperation in an experimental microbial metapopulation. Proceedings of the National Academy of Sciences of the USA 110:7354–7359.

Sheik, C. S., W. H. Beasley, M. S. Elshahed, X. H. Zhou, Y. Q. Luo, and L. R. Krumholz. 2011. Effect of warming and drought on grassland microbial communities. ISME Journal 5:1692–1700.

Sibly, R. M., T. D. Williams, and M. B. Jones. 2000. How environmental stress affects density dependence and carrying capacity in a marine copepod. Journal of Applied Ecology 37:388–397.

Skellam, J. G. 1951. Random dispersal in theoretical populations. Biometrika 38:196–218.

Solis-Weiss, V., F. Aleffi, N. Bettoso, P. Rossin, G. Orel, and S. Fonda-Umani. 2004. Effects of industrial and urban pollution on the benthic macrofauna in the Bay of Muggia (industrial port of Trieste, Italy). Science of the Total Environment 328:247–263.

Spromberg, J. A., B. M. John, and W. G. Landis. 1998. Metapopulation dynamics: indirect effects and multiple distinct outcomes in ecological risk assessment. Environmental Toxicology and Chemistry 17:1640–1649.

Tilman, D. 1982. Resource competition and community structure. Princeton University Press, Princeton, NJ.

Tilman, D., and C. Lehman. 2001. Human-caused environmental change: impacts on plant diversity and evolution. Proceedings of the National Academy of Sciences of the USA 98:5433–5440.

Van Dyken, J. D., and B. Zhang. 2019. Carrying capacity of a spatially-structured population: disentangling the effects of dispersal, growth parameters, habitat heterogeneity and habitat clustering. Journal of Theoretical Biology 460:115–124.

Wang, Y. S., and D. L. DeAngelis. 2019. Energetic constraints and the paradox of a diffusing population in a heterogeneous environment. Theoretical Population Biology 125:30–37.

Wilson, J. R. U., E. E. Dormontt, P. J. Prentis, A. J. Lowe, and D. M. Richardson. 2009. Something in the way you move: dispersal pathways affect invasion success. Trends in Ecology and Evolution 24:136–144.

Wright, S. 1943. Isolation by distance. Genetics 28:114–138.
Yao, Y., L. Tuduri, T. Harner, P. Blanchard, D. Waite, L. Poissant, C. Murphy, et al. 2006. Spatial and temporal distribution of pesticide air concentrations in Canadian agricultural regions. Atmospheric Environment 40:4339–4351.
Zhang, B, D. L. DeAngelis, W.-M. Ni, Y. Wang, L. Zhai, A. Kula, S. Xu, and J. D. Van Dyken. 2020. Effect of stressors on the carrying capacity of spatially distributed metapopulations. American Naturalist, Dryad Digital Repository, https://doi.org/10.25338/B8090K.
Zhang, B., A. Kula, K. M. L. Mack, L. Zhai, A. L. Ryce, W. M. Ni, D. L. DeAngelis, et al. 2017. Carrying capacity in a heterogeneous environment with habitat connectivity. Ecology Letters 20:1118–1128.
Zhang, B., X. Liu, D. L. DeAngelis, W. M. Ni, and G. G. Wang. 2015. Effects of dispersal on total biomass in a patchy, heterogeneous system: analysis and experiment. Mathematical Biosciences 264:54–62.

Associate Editor: Volker Grimm
Editor: Russell Bonduriansky

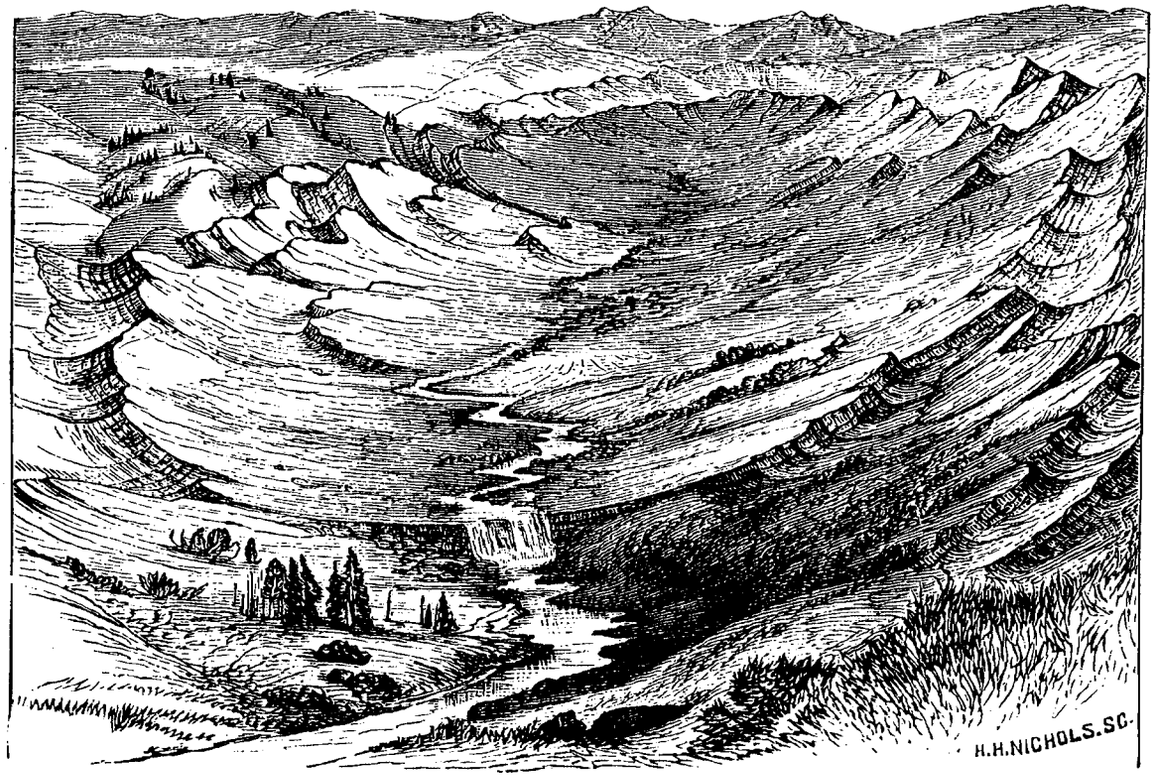

"A synclinal valley." From the review of Powell's *Exploration of the Colorado River* (*The American Naturalist*, 1876, 10:736–739).